



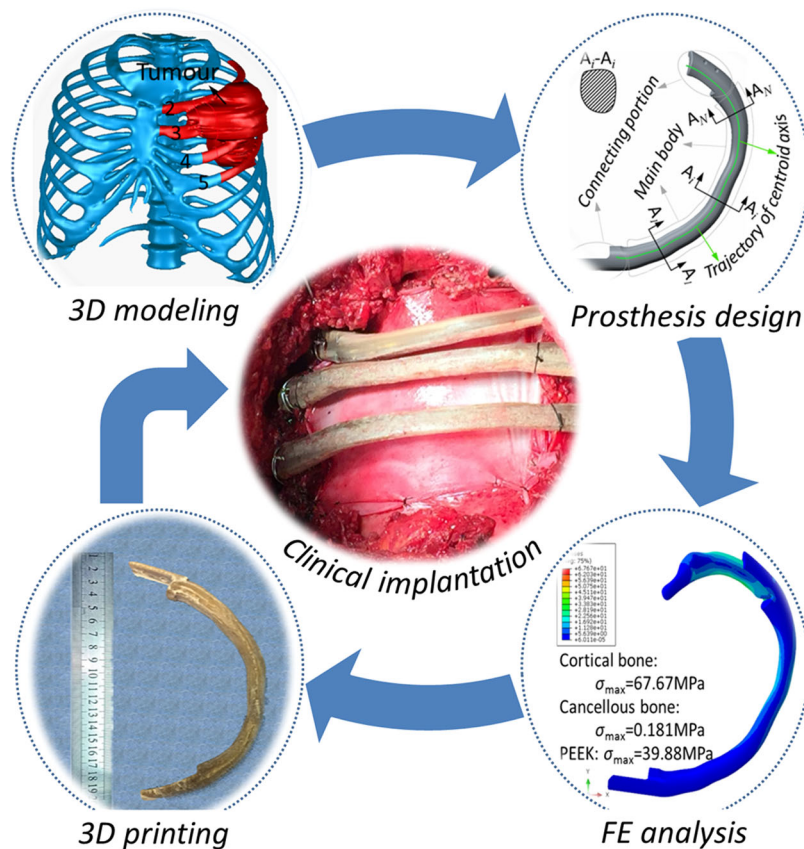
Custom design and biomechanical analysis of 3D-printed PEEK rib prostheses

Jianfeng Kang¹ · Ling Wang¹ · Chuncheng Yang¹ · Lei Wang² · Cao Yi¹ · Jiankang He¹ · Dichen Li¹

Received: 13 November 2017 / Accepted: 2 April 2018 / Published online: 5 May 2018
© The Author(s) 2018

Abstract A tumour resection normally involves a large tissue resection and bone replacement. Polyether ether ketone (PEEK) has become a suitable candidate for use in various prostheses owing to its lightness in weight, modulus close to that of natural bone, and good biocompatibility, among other factors. This study proposes a new design method for a rib prosthesis using the centroid trajectory of the natural replaced rib, where the strength can be adjusted by monitoring the cross-sectional area, shape, and properties. A custom-designed rib prosthesis was manufactured using fused deposition modelling (FDM) manufacturing technology, and the mechanical behaviour was found to be close to that of a natural rib. A finite element analysis of the designed rib was carried out under similar loading conditions to those used in mechanical testing. The results indicate that the centroid trajectory derived from a natural rib diaphysis can provide reliable guidance for the design of a rib prosthesis. Such methodology not only offers considerable design freedom in terms of shape and required strength, but also benefits the quality of the surface finishing for samples manufactured using the FDM technique. FDM-printed PEEK rib prostheses have been successfully implanted, and good clinical performances have been achieved.

Graphical abstract



Keywords Custom design · Biomechanical analysis · Polyether ether ketone (PEEK) · Rib prostheses · 3D printing

1 Introduction

Chest wall resections are often required when dealing with malignant tumours, congenital deformities, or thoracic injuries from vehicle crashes, and may lead to the risk of a rib excision. Moreover, rib fractures are significantly increasing as the global population continues to age. Herein, the development of human rib replacement techniques has received significant attention in terms of chest wall reconstructions as a way to maintain the normal respiratory function of patients (Moradiellos et al. 2017; Simal et al. 2016; Wang et al. 2016; Wu et al. 2016).

Many different materials have been used thus far to fabricate rib prostheses, including polytetrafluoroethylene or a polypropylene mesh (Weyant et al. 2006), polymethylmethacrylate and its composites (Agrawal et al. 1998; Vartanian et al. 2006), stainless steel, and titanium or titanium-based alloys (Bille et al. 2012; Gonfiotti et al. 2009; Stephenson et al. 2011). In addition, with the rapid development of 3D printing technology, custom-designed titanium implants have become favourable owing to their excellent biocompatibility and features (Anderson et al. 2016; Aragon and Perez 2016; Aranda et al. 2015; Moradiellos et al. 2017; Rungsiyakull et al. 2015; Simal et al. 2016; Wang et al. 2016). However, statistical results have shown a relatively high incidence rate of post-operative complications (Weyant et al. 2006), reaching up to 27% for massive chest wall defects (Berthet et al. 2012). Moreover, relevant studies (Hazel and Weyant 2015; Weyant et al. 2006) have indicated that respiratory failure may be related to the choice of rigid repair for such defects. As a result of the significant differences in elastic modulus or toughness between titanium rib implants and real human ribs, the stress distributions of the rib skeleton will be changed after a rib cage replacement, and a non-uniform load transmission may cause damage to the surrounding organs under certain unique circumstances, including a tumble or slight impact. Moreover, titanium has a limitation with regard to post-operative imaging examinations owing to the presence of artefacts (Smeets et al. 2017). Unfortunately, some patients may feel abnormal symptoms near the replacement location when titanium alloy is used (Fage et al. 2016). Therefore, improvements in the clinical performance of prostheses and a reduction in the incidence rate of post-operative complications through the use of better-suited biomaterials and a subject-specific design are still required.

Polyether ether ketone (PEEK) has been widely used for spinal fusions (Tanida et al. 2016) and cranioplasty (Garcia-Gonzalez et al. 2015) owing to its excellent biomechanical properties, biocompatibility, and stability, particularly its comparable elastic modulus to that of bone. However, studies on rib prostheses with PEEK materials have been limited. In this paper, a general prostheses design procedure is described for patient-specific rib prostheses printed using PEEK through a fused deposition modelling (FDM) technique. Preoperative planning was carried out to determine the position of the tumour resection, and the geometrical model of the replaced rib was reconstructed. A new methodology for designing rib prostheses was introduced, and the centroid trajectory of a natural rib was specifically extracted and used as a guideline for a rib prosthesis design, which is called the C-design. For comparison purposes, a traditional methodology for a rib design based on the original defect model (D-design) was also constructed. The biomechanical behaviours for a natural rib, D-design prosthesis, and C-design prosthesis under similar critical rib fracture conditions were analysed using the finite element method (FEM), and then validated through mechanical testing of rib samples fabricated using FDM. A clinical case report proved the successful application of such prosthesis with good stability and post-operative performance.

2 Materials and method

2.1 Clinical data and preoperative planning

A 43-year-old male patient in Tangdu hospital (the Second Affiliated Hospital of the Fourth Military Medical University, Shaanxi, China) complained of prolonged chest pain and was diagnosed as having chondrosarcoma. A CT scan showed a large tumour (11 cm × 11 cm × 6 cm) located in the left chest wall, which had invaded the second through fifth ribs, as shown in Fig. 1. For a better observation and prosthesis design, using Mimics software (version 16.0, Materialise, Inc., Leuven, Belgium), a 3D model of the chest was constructed from the CT data, and the tumour and corresponding ribs were planned for resection under the premise of ensuring a negative margin of 30 mm (Moradiellos et al. 2017; Wu et al. 2016). Owing to the existence of costal cartilaginous tissue at the connection points of the second and third ribs after a full resection, the two rib prostheses needed to be fixed to the corpus sterni using titanium screws or a steel wire, and the remaining prostheses, the connections of which were designed in a C shape, were tied to the surface of the adjacent residual ribs. The assembly of all rib prostheses and thoracic skeletons can be imitated to verify the feasibility of the prostheses and detect the effects of clinical implantation.

✉ Ling Wang
menlwang@mail.xjtu.edu.cn

¹ State Key Laboratory for Manufacturing Systems Engineering, Xi'an Jiaotong University, Xi'an, Shaan Xi, China

² Departments of Thoracic Surgery, Tangdu Hospital, The Fourth Military Medical University, Xi'an, Shaan Xi, China

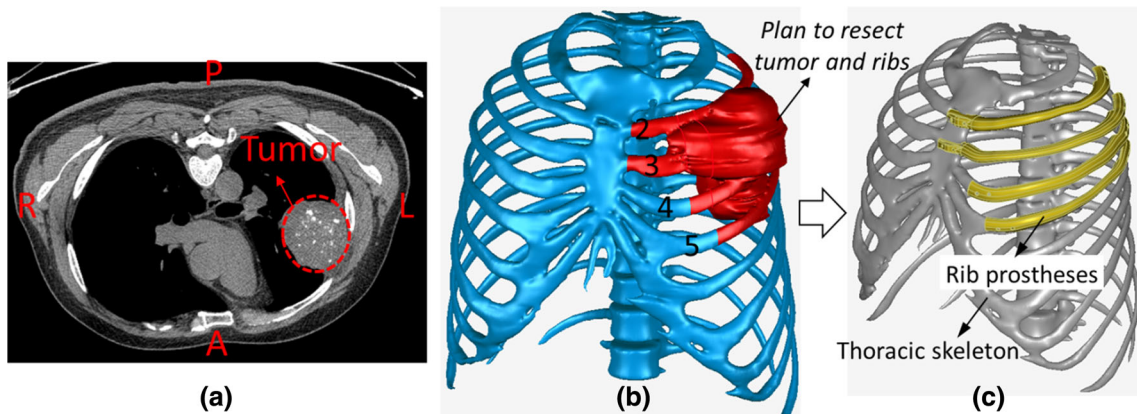


Fig. 1 Patient preoperative planning: **a** tumour position in the CT image, **b** resection plan of tumour and corresponding ribs, and **c** chest wall reconstruction using PEEK rib prostheses

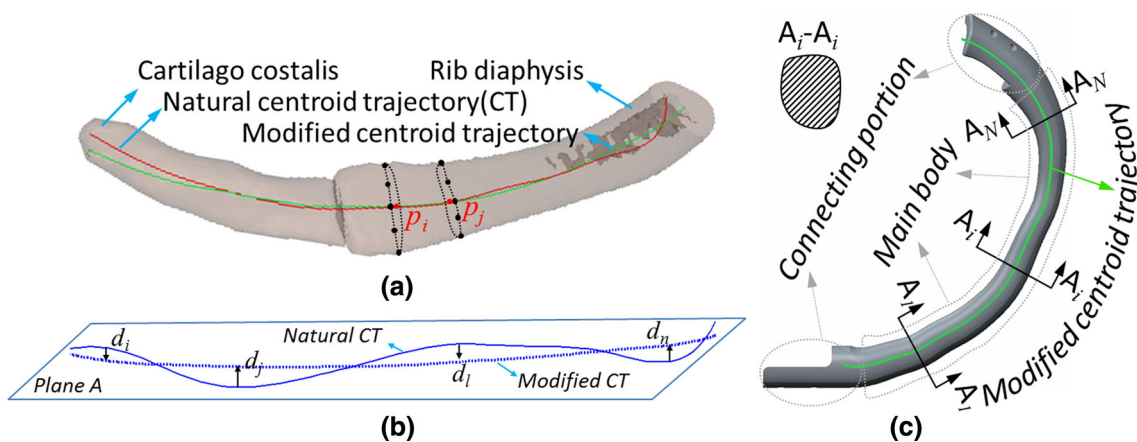


Fig. 2 Design flow for customized rib prosthesis: **a** extraction of centroid trajectory, **b** modification of centroid trajectory, and **c** generation of prosthesis

2.2 Design of rib prosthesis

According to the anatomical structure of a natural rib, the profile of the cross section in the middle part of the rib is approximately elliptical in shape, whereas the front and rear ends are slightly thick and flat. The traditional design method of rib prosthesis is to keep the implant identical to that of the natural tissue. Although this design makes the volume and weight of the prostheses close to their demand, the surface topological properties of the natural rib will contribute significantly to the stair-stepping effect in the FDM printing process (Chakraborty et al. 2008; Chohan et al. 2017; Nelaturi and Shapiro 2015). Moreover, removing the additional support structures may cause microcracks on the surface and affect the overall service performance. To solve the above problems and improve the comprehensive performances of prosthesis, a new rib prosthesis design method was developed based on the centroid trajectory of a natural rib diaphysis and variable section sweep (VSS). The prostheses models are called centroid design (C-design) models.

The main flows of the prosthesis design include three aspects: extraction of the centroid trajectory for the natural ribs and cartilago costalis, modification of the centroid trajectory owing to the influences of manufacturing factors, and generation of the main body of the prosthesis through a VSS along the centroid trajectory and the connection design. As shown in Fig. 2, the natural centroid trajectory was extracted using a smoothing curve successively connecting the centres of all cross sections. The centre coordinate $P_i(x_i, y_i, z_i)$ can be calculated from all discrete points of the cross-sectional profile, as expressed in Eq. 1:

$$\bar{x}_i = \frac{1}{n_p} \sum_{k=1}^{n_p} x_i; \bar{y}_i = \frac{1}{n_p} \sum_{k=1}^{n_p} y_i; \bar{z}_i = \frac{1}{n_p} \sum_{k=1}^{n_p} z_i \tag{1}$$

where n_p represents the total numbers of discrete points for the cross-sectional profile.

The natural centroid trajectory (Fig. 2a) exhibits the spatial non-uniplanar distribution law owing to the influence of heterogeneous and irregular cross sections for natural ribs

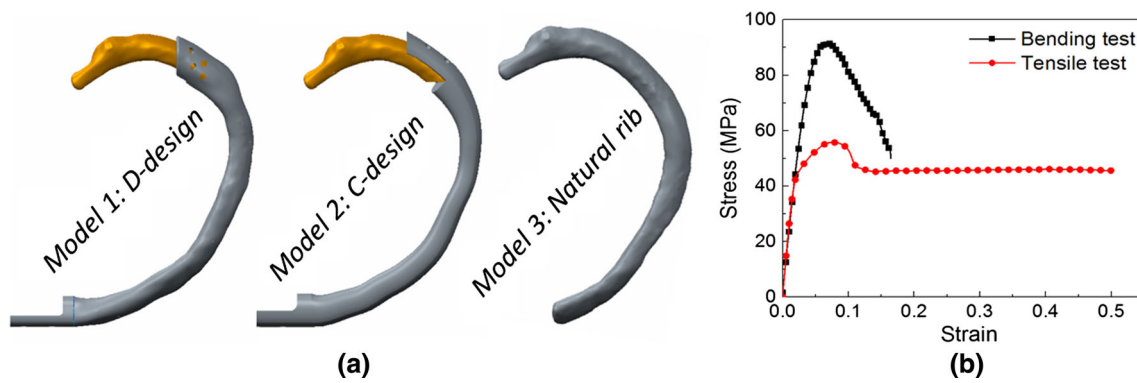


Fig. 3 **a** Different models for finite element analysis and **b** finite element mesh

Table 1 Material properties of the components used in finite element analysis

Components	Elastic modulus (GPa)	Poisson's ratio	Tensile strength (MPa)	Flexural strength (MPa)	References
Cortical bone	12	0.3	88	76.0 ± 23.7	(Li et al. 2010a, b)
Cancellous bone	0.04	0.45	2.2	/	
PEEK rib prosthesis	2.8	0.3	89	141	(Yang et al. 2017)

and cartilago costalis. For an improvement in the surface quality, the geometric corrections in the coplanar are applied to modify the natural centroid trajectory. The objective of coplanar processing is to find a spatial plane to minimize the sum of squares of the distance from the centres of the cross section to the plane. As shown in Fig. 2b, it is assumed that a spatial plane exists, the function equation of which is $z = f(x, y) = a_0x + a_1y + a_2$. Therefore, the sum of the squares of the distance can be calculated as follows:

$$S = \sum_{i=0}^n (a_0\bar{x}_i + a_1\bar{y}_i + a_2 - \bar{z}_i)^2$$

Based on the extreme value theory, when the partial derivatives for function S are equal to zero, the minimum exists. That is, $\frac{\partial S}{\partial a_k} = 0$, ($k = 0, 1, 2$). All parameters of the plane equation can be obtained by solving the system of linear equations. Finally, the natural centroid trajectory is projected onto the plane to finish the coplanar modification.

A variable cross-sectional area is assigned along the derived centroid trajectory to be adaptive to the natural rib tissue using linear interpolation methods, applying the variable section scanning function in the Creo software (version 2.0, Parametric Technology, Co., USA). For a fixation of a rib prosthesis, when the prosthesis is attached to the remaining rib, the connecting portion usually needs to extend 20–30 mm from the osteotomy surface. Moreover, a larger contact area and good matching of the interface between the prosthesis and rib diaphysis are taken as priorities under sufficient

strength. A geometric model and the design flows for the second rib prostheses are shown in Fig. 2c.

2.3 Biomechanical analysis of rib prosthesis

The FEM was used to investigate the biomechanical properties of the rib prostheses designed using the method presented in this study. Meanwhile, to evaluate the comprehensive performances of the prosthesis, the direct design (D-design) model and a natural rib model were analysed and compared with the C-design model, as shown in Fig. 3a. The D-design model was constructed through a repair of the surface morphology of resected ribs, and a design of the fixed structure at both ends. Geometric versions of the three models were generated through the processing of CT images using the software Mimics and a smoothing operation using the software Geomagic Studio (version 2012, Geomagic, Inc., USA), and assembled according to the preoperative planning. In this modelling process, the rib includes cortical bone and cancellous bone, and the thickness of the cortical bone is approximately 0.7 mm, based on (Li et al. 2010a; Mohr et al. 2007).

All material properties used in the finite element analysis were set as given in Table 1. To reduce the influences from manufacturing methods and FDM process parameters, the material properties of the PEEK rib prostheses were defined based on the results of the tensile and flexure tests, which were conducted using an electrohydraulic servo mechanical testing machine (SANS CMT4304, MTS Corp., USA) according to ISO 527-1:2012 and ISO 178, respectively. All

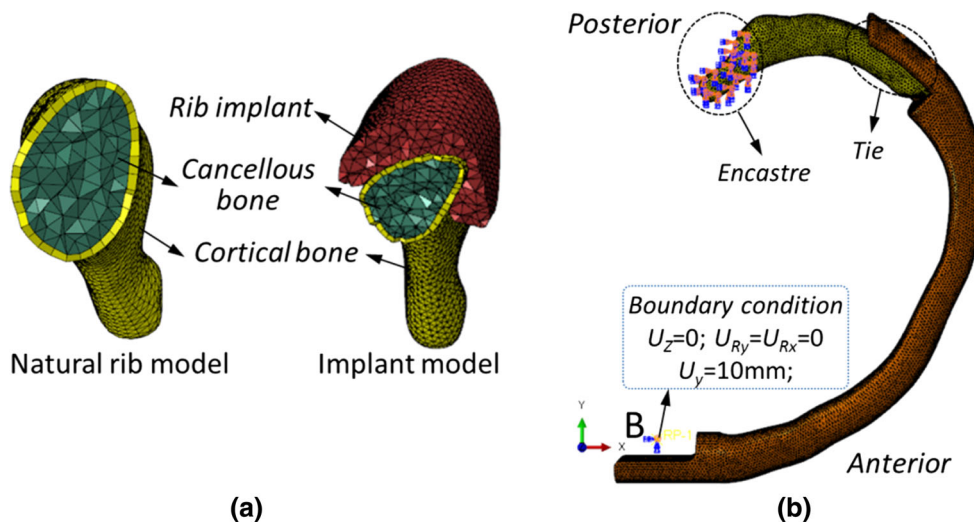


Fig. 4 Loading and boundary conditions for finite element model

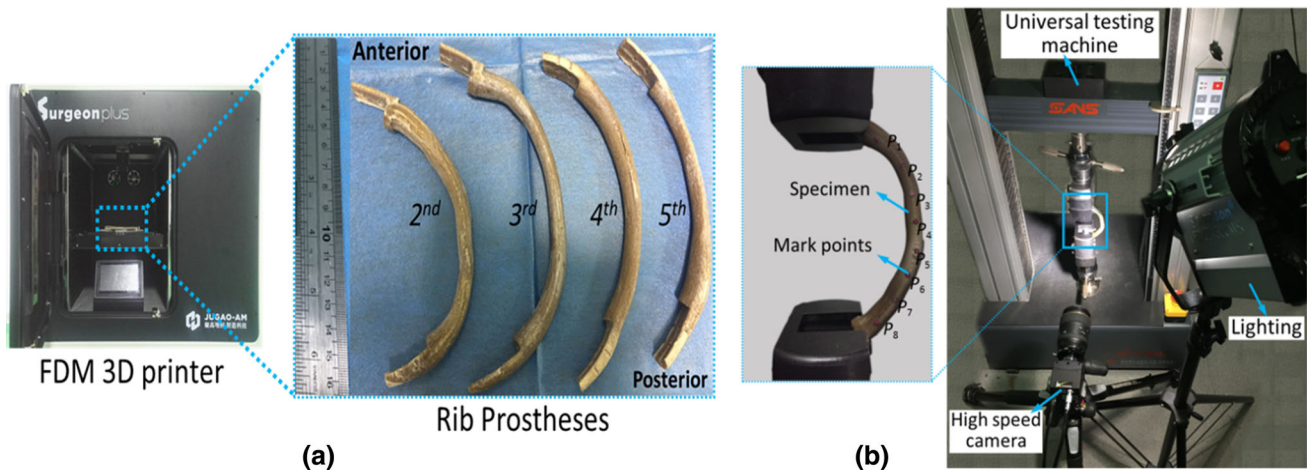


Fig. 5 a Custom-designed rib prostheses and b configuration of the bending test

materials were assumed to be homogeneous, isotropic, and linear elastic.

Three element sizes were used for the mesh sensitivity analysis: 0.25, 0.5, and 1 mm. A relative difference of less than 5% was achieved across all sizes; thus, 1 mm was selected as the overall meshing size for this study. As shown in Fig. 4a, three geometric models were meshed automatically using Hypermesh (version 12, Altair Engineering, Inc., USA) with an element size of 1 mm and applying a C3D6 element type, and then solved in Abaqus (version 14, Abaqus, Inc., USA). The outer cortical shells for each rib were modelled using an inward offset with a thickness of 0.7 mm. The contact interface between the prosthesis and rib was considered rigidly bonded to simulate the fixation with a titanium screw or steel wire. Because it is very difficult to evaluate the load-bearing capacity of each natural rib *in vivo*, this study mainly investigated the biomechanical properties under the extreme conditions of a rib fracture. The posterior extremity

of the rib near the transverse process was fully fixed. For the anterior extremity or connector of the rib prostheses bounding on the sternal body, the translation (U_z) or rotation (U_{Ry} & U_{Rx}) out of the loading plane XOY was constrained; nevertheless, the rotational degree of freedom around the vertical axis was released, as shown in Fig. 4b. A displacement loading of 10 mm instead of a force loading was applied to the anterior extremity (B) of the rib model along the vertical axis (Y axis), representing the general compressive loading direction of a chest when being punched (Li et al. 2010a, b).

The designed specimens were 3D printed using the FDM technique with a self-developed 3D printer created specifically for PEEK printing (Fig. 5a), with the nozzle diameter of 0.4mm, printing speed of 40mm/s, printing line width of 0.4mm, layer thickness of 0.2mm, nozzle temperature of 420°C, infill percentage of 100% and printing trajectories of the contour offset scan. The printing direction is perpendicular to the position of prosthesis in Fig. 5a. To evaluate

the bending performance of the printed samples and validate the finite element models, a bending test was carried out for the 3D-printed rib prosthesis using a universal testing machine, as shown in Fig. 5b. Both ends of the prosthesis were clamped, and a vertical displacement of 10 mm was applied through the top fixture point at a speed of 1 mm/min. Markers were attached to the surface of the rib prosthesis beforehand, and a deformation of the rib prosthesis was obtained by capturing the moving trajectory of the marked points using a high-speed camera (i-Speed 3, Olympus KeyMed, Ltd., UK). Finally, a comparison of the results between the FEA and experimental testing was conducted to comprehensively evaluate the mechanical properties of the rib prosthesis.

3 Results

The results of Mises stresses and displacement for the second rib model are shown in Fig. 6a. Among the three finite element models, the maximum von Mises stress of the cortical bone in the natural rib model reached up to 143.7 MPa, which was twice that of the other two prosthesis models, and exceeded the tensile yield strength (88 MPa) and bending strength (76.0 ± 23.7 MPa) of cortical bone. Meanwhile, the maximum von Mises stress of cancellous bone was over the yield strength of the material (2.2 MPa), which may lead to a high risk of fracture in the maximum stress position. The patterns of stress distribution in the rib model predicted for the two prostheses were similar to each other, and the magnitudes of the maximum von Mises stresses also matched well. Regardless, the maximum von Mises stresses predicted for all model types were below the yield strength limitation of the materials. For the PEEK parts, the maximum von Mises stress predicted for the C-designed model was 39.88 MPa, which was 10% larger than those of the D-design model, but lower than the tensile yield strength and the bending strength of the PEEK material. In addition, as shown in Fig. 6b, the initial stiffness of natural rib calculated by FEA is close to the experimental result from the references (Li et al. 2010), and so do the stiffness of two kinds of prostheses. However, the stiffness of prosthesis is larger than that of natural rib owing to the difference of elastic modulus between cortical bone and PEEK materials.

The experimental results of the bending test for the 3D-printed PEEK rib prosthesis (Fig. 7) show that the displacement reaches the maximum level at around the middle point (P_5), and decreases gradually towards both ends, which follows a pattern similar to that of the FEA. However, the difference in deformation between the FEA and experimental test can reach up to 20%.

The patient underwent a complete tumour resection, and the second and fifth ribs were partly resected according to

the preoperative planning strategy. The size of the chest wall defect reached 20 cm \times 15 cm. Compared to the 558 g tumour specimen, the weight of each PEEK rib prosthesis was approximately 27 g, and the total weight was approximately 100 g. Because the fifth ribs were simply cut off from a very short part, three rib prostheses were used during the clinical operation, as shown in Fig. 8. The patient was discharged 10 days after surgery, and a chest CT scan indicated a stable reconstruction, with a preservation of the thoracic morphology and excellent cosmetic results.

4 Discussion

A tumour around the chest occasionally involves a large tissue resection, including the ribs, and to reconstruct the chest wall, it is necessary to design and manufacture a biomimetic rib prosthesis mimicking natural ribs. To realize such a goal, a methodology was developed to reconstruct a rib prosthesis model based on the derived centroid trajectory of the natural rib being replaced. This methodology was specially designed to benefit one of the 3D printing techniques, namely, FDM, to minimize artefacts called “stepping”. The FEM was used to analyse the biomechanical behaviour of such designed rib prostheses and was validated experimentally.

Compared with metal prostheses (Aragon and Perez 2016; Fraldi et al. 2010; Simal et al. 2016; Wang et al. 2016), PEEK exhibits excellent biocompatibility, the Young’s modulus and yield strength of which match those of cortical bone. Such advantages make PEEK a better candidate for spinal fusion cage and cranioplasty implants (Garcia-Gonzalez et al. 2015; Tan et al. 2016; Tanida et al. 2016). This is the first study wherein PEEK was fabricating rib prosthesis. Owing to the uniform stress transmission between the prosthesis and rib, a PEEK rib prosthesis was strongly fastened to a remaining rib, and offered better stability and safety for certain unexpected situations, such as a tumble or slight impact. Moreover, high radiographic penetrability can effectively avoid interference from artefacts during a post-operative examination. Therefore, PEEK can be a preferred material for a rib prosthesis.

The traditional design of rib prosthesis is based on the original surface geometric characteristics of the natural rib, which is also called a reverse engineering methodology. However, the topological surface properties of a natural rib can contribute significantly to a stair-stepping effect during the manufacturing process of FDM printing (Chakraborty et al. 2008; Chohan et al. 2017). In this study, a new methodology was developed for the design of a patient-specific PEEK rib prosthesis based on the centroid trajectory of the replaced rib. The methodology was validated through a comparison to a traditional design model using the FEA and mechanical testing on the printed rib samples based on the FDM methodology. The maximum Mises stress predicted

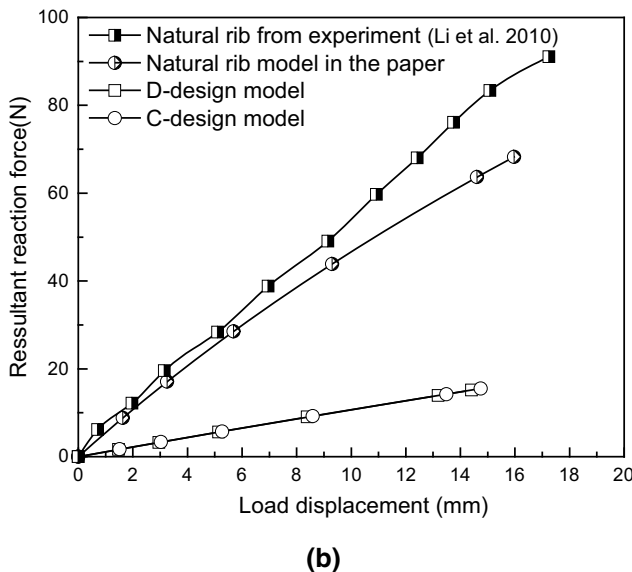
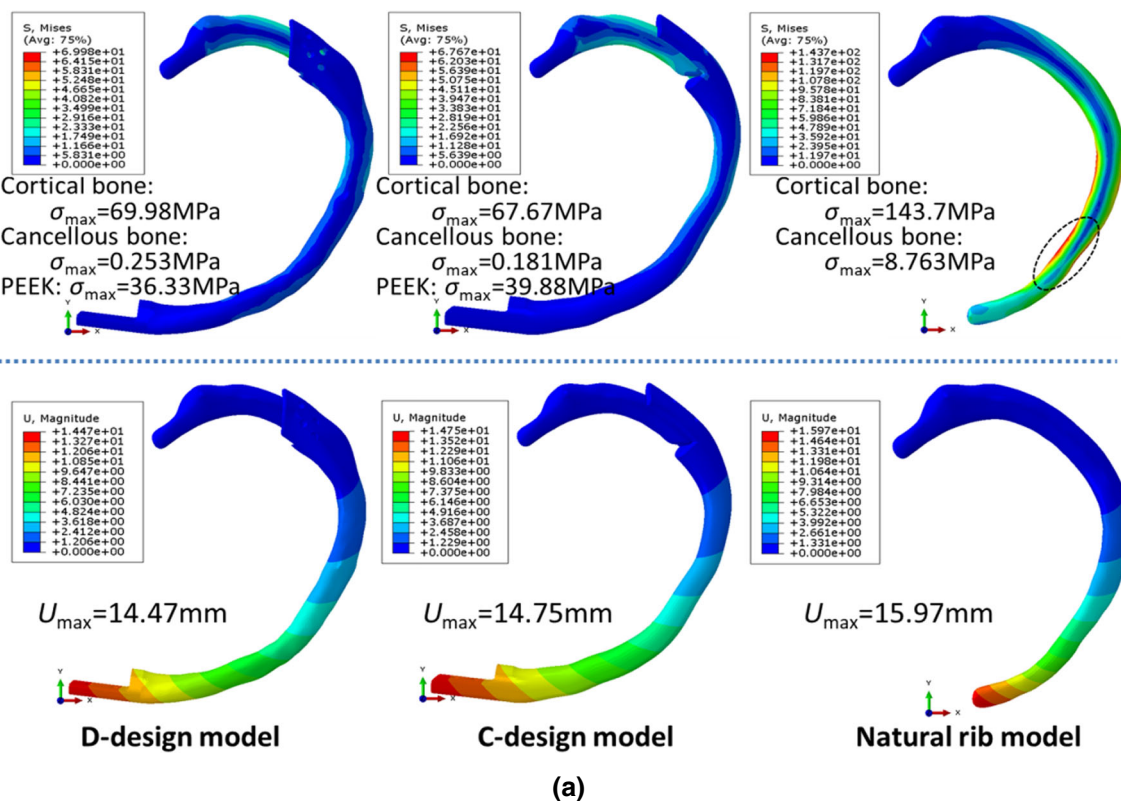


Fig. 6 **a** Contour plot of von Mises stress and displacement predicted for three models corresponding to three designs; **b** the load-displacement curve of different models

using FEA occurred in the middle region of the rib model for both designs, and both were found to be lower than the yield strength of the PEEK materials. This indicates that both designed prostheses can meet the strength requirement of ribs during normal daily life. In addition, the maximal von Mises stress of the C-design prosthesis was 10% larger than that of the D-design, which may result from the difference in cross-

sectional areas for both designs. A larger cross-sectional area is associated with a higher strength but lower stiffness of the rib prosthesis, and therefore, the strength and stiffness can be adjusted for the C-design prosthesis by controlling the variation in the cross-sectional area, which offers better design freedom compared to the D-design method.

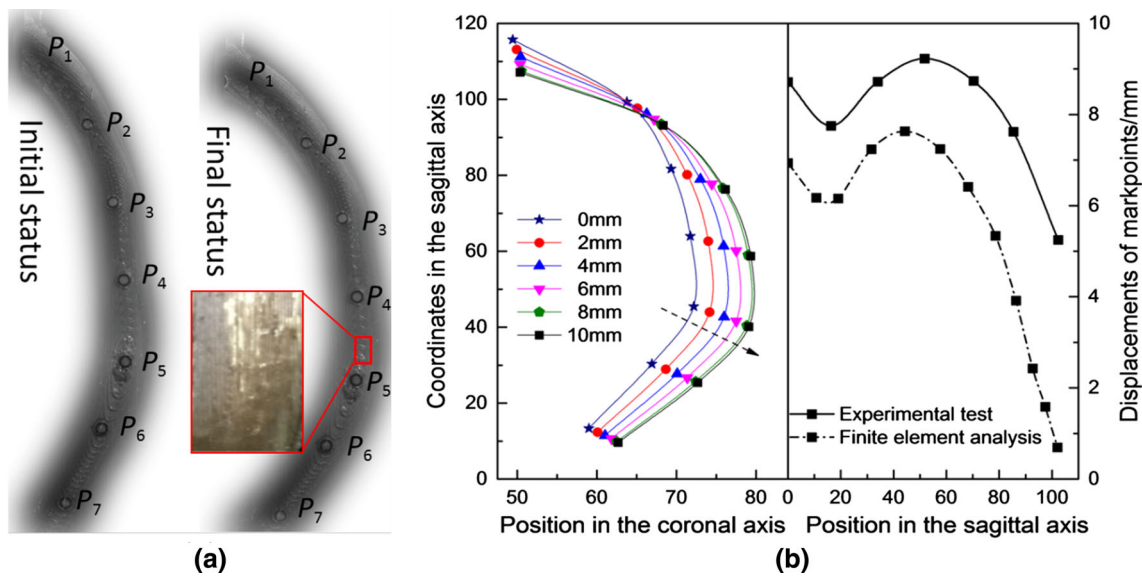


Fig. 7 **a** Experimental results for the bending test, and **b** the variation rule of displacement for the 3D-printed PEEK rib prosthesis under the different loads (left), as well as a comparison of displacement between the experimental test and FEA under similar critical conditions of a natural rib fracture (right)

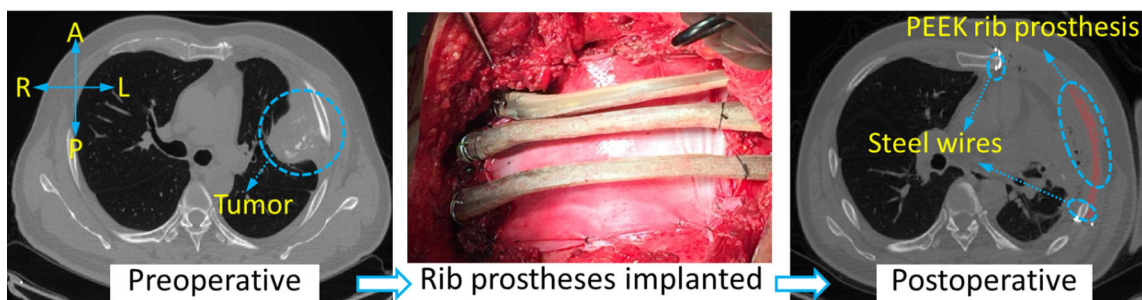


Fig. 8 Clinical implantation and post-operative effect of rib prosthesis

Meanwhile, the biomechanical evaluation of a 3D-printed PEEK rib prosthesis was validated through experimental tests. The rule of displacement variation of PEEK rib prosthesis was consistent with that of the FEA, and no microcracking was observed at the position of maximal deformation throughout the bending test. Although the displacement error between the FEA and experimental test was up to 20%, overall, these results indicate that a 3D-printed PEEK rib prosthesis can fully meet the performance requirements. The possible causes of this difference are numerous, with one being that the crystallinity of the polymer affected the material properties, such as the yield strength and roughness (Yang et al. 2017). In addition, factors including the surface roughness and dimensional mismatch can contribute to the difference between the FEA and mechanical testing results (Wang et al. 2017). Therefore, it is necessary to validate the actual mechanical properties for the purposes of application and referencing. Moreover, a completed thorax with an implanted prosthesis needs to be analysed further

under *in vivo* loading conditions for better characterizing the comprehensive mechanical behaviours of rib prosthesis.

5 Conclusion

A new methodology was developed for the design of a patient-specific PEEK rib prosthesis that is particularly suitable for the FDM manufacturing technique. The results indicate that the centroid trajectory derived from a natural rib diaphysis can provide reliable guidance for a rib prosthesis design. Moreover, the newly developed methodology offers high freedom of design in terms of the cross-sectional area and shape. The designed rib prostheses were manufactured using FDM technology, and the mechanical behaviours of which were found to be close to those of natural ribs. PEEK rib prostheses were implanted successfully, and a good clinical performance was achieved.

Acknowledgements This work was supported by Fundamental Research Funds for the Central Universities and the Program of International

Scientific & Technological Cooperation and Exchange Planning in Shaanxi Province (606222147063). Samples were provided by JuGao.

Compliance with ethical standards

Conflict of interest The authors listed in this manuscript have no conflicts of interest to declare.

Open Access This article is distributed under the terms of the Creative Commons Attribution 4.0 International License (<http://creativecommons.org/licenses/by/4.0/>), which permits unrestricted use, distribution, and reproduction in any medium, provided you give appropriate credit to the original author(s) and the source, provide a link to the Creative Commons license, and indicate if changes were made.

References

- Agrawal K, Subbarao KS, Nachiappan M, Arumugam A (1998) An innovative method of reconstruction of large skeletal chest wall defects. *Plast Reconstr Surg* 102:839–842. <https://doi.org/10.1097/00006534-199809030-00035>
- Anderson CJ, Spruiell MD, Wylie EF, McGowan CM, Deleyiannis FWB, Donaldson NJ, Heare TC (2016) A technique for pediatric chest wall reconstruction using custom-designed titanium implants: description of technique and report of two cases. *J Child Orthop* 10:49–55. <https://doi.org/10.1007/s11832-015-0709-1>
- Aragon J, Perez Mendez I (2016) Dynamic 3D printed titanium copy prosthesis: a novel design for large chest wall resection and reconstruction. *J Thorac Dis* 8:385–389. <https://doi.org/10.21037/jtd.2016.03.94>
- Aranda JL, Jimenez MF, Rodriguez M, Varela G (2015) Tridimensional titanium-printed custom-made prosthesis for sternocostal reconstruction. *Eur J Cardio Thorac Surg Off J Eur Assoc Cardio Thorac Surg* 48:92–94. <https://doi.org/10.1093/ejcts/ezv265>
- Berthet JP et al (2012) The combination of polytetrafluoroethylene mesh and titanium rib implants: an innovative process for reconstructing large full thickness chest wall defects. *Eur J Cardio Thorac Surg Off J Eur Assoc Cardio Thorac Surg* 42:444–453. <https://doi.org/10.1093/ejcts/ezs028>
- Bille A, Okiror L, Karenovics W, Routledge T (2012) Experience with titanium devices for rib fixation and coverage of chest wall defects. *Interact Cardiovasc Thorac Surg* 15:588–595. <https://doi.org/10.1093/icvts/ivs327>
- Chakraborty D, Reddy BA, Choudhury AR (2008) Extruder path generation for curved layer fused deposition modeling. *Comput Aided Des* 40:235–243. <https://doi.org/10.1016/j.cad.2007.10.014>
- Chohan JS, Singh R, Boparai KS, Penna R, Fraternali F (2017) Dimensional accuracy analysis of coupled fused deposition modeling and vapour smoothing operations for biomedical applications. *Compos Part B Eng* 117:138–149. <https://doi.org/10.1016/j.compositesb.2017.02.045>
- Fage SW, Muris J, Jakobsen SS, Thyssen JP (2016) Titanium: a review on exposure, release, penetration, allergy, epidemiology, and clinical reactivity. *Contact Dermat* 74:323–345. <https://doi.org/10.1111/cod.12565>
- Fraldi M, Esposito L, Perrella G, Cutolo A, Cowin SC (2010) Topological optimization in hip prosthesis design. *Biomech Model Mechanobiol* 9:389–402. <https://doi.org/10.1007/s10237-009-0183-0>
- García-González D, Rusinek A, Jankowiak T, Arias A (2015) Mechanical impact behavior of polyether-ether-ketone (PEEK). *Compos Struct* 124:88–99. <https://doi.org/10.1016/j.compstruct.2014.12.061>
- Gonfiotti A, Santini PF, Campanacci D, Innocenti M, Ferrarello S, Janni A (2009) Use of moldable titanium bars and rib clips for total sternal replacement: a new composite technique. *J Thorac Cardiovasc Surg* 138:1248–1250. <https://doi.org/10.1016/j.jtcvs.2008.09.034>
- Hazel K, Weyant MJ (2015) Chest wall resection and reconstruction: management of complications. *Thorac Surg Clin* 25:517–521. <https://doi.org/10.1016/j.thorsurg.2015.07.013>
- Li Z, Kindig MW, Kerrigan JR, Untaroiu CD, Subit D, Crandall JR, Kent RW (2010a) Rib fractures under anterior-posterior dynamic loads: experimental and finite-element study. *J Biomech* 43:228–234. <https://doi.org/10.1016/j.jbiomech.2009.08.040>
- Li Z, Kindig MW, Subit D, Kent RW (2010b) Influence of mesh density, cortical thickness and material properties on human rib fracture prediction. *Med Eng Phys* 32:998–1008. <https://doi.org/10.1016/j.medengphy.2010.06.015>
- Mohr M, Abrams E, Engel C, Long WB, Bottlang M (2007) Geometry of human ribs pertinent to orthopedic chest-wall reconstruction. *J Biomech* 40:1310–1317. <https://doi.org/10.1016/j.jbiomech.2006.05.017>
- Moradiellos J, Amor S, Cordoba M, Rocco G, Vidal M, Varela A (2017) Functional chest wall reconstruction with a biomechanical three-dimensionally printed implant. *Ann Thorac Surg* 103:389–391. <https://doi.org/10.1016/j.athoracsur.2016.11.048>
- Nelaturi S, Shapiro V (2015) Representation and analysis of additively manufactured parts. *Comput Aided Des* 67–68:13–23
- Rungsiyakull C, Chen J, Rungsiyakull P, Li W, Swain M, Li Q (2015) Bone's responses to different designs of implant-supported fixed partial dentures. *Biomech Model Mechanobiol* 14:403–411. <https://doi.org/10.1007/s10237-014-0612-6>
- Simal I et al (2016) Three-dimensional custom-made titanium ribs for reconstruction of a large chest wall defect. *Eur Pediatr Surg Rep* 4:26–30. <https://doi.org/10.1055/s-0036-1593738>
- Smeets R et al (2017) Artefacts in multimodal imaging of titanium, zirconium and binary titanium-zirconium alloy dental implants: an in vitro study. *Dentomaxillofacial Radiol*. <https://doi.org/10.1259/dmfr.20160267>
- Stephenson JT, Song K, Avansino JR, Mesher A, Waldhausen JH (2011) Novel titanium constructs for chest wall reconstruction in children. *J Pediatr Surg* 46:1005–1010. <https://doi.org/10.1016/j.jpedsurg.2010.12.007>
- Tan ET, Ling JM, Dinesh SK (2016) The feasibility of producing patient-specific acrylic cranioplasty implants with a low-cost 3D printer. *J Neurosurg* 124:1531–1537. <https://doi.org/10.3171/2015.5.JNS15119>
- Tanida S, Fujibayashi S, Otsuki B, Masamoto K, Takahashi Y, Nakayama T, Matsuda S (2016) Vertebral endplate cyst as a predictor of nonunion after lumbar interbody fusion comparison of titanium and polyetheretherketone. *Cages Spine* 41:1216–1222. <https://doi.org/10.1097/brs.0000000000001605>
- Vartanian SM, Colaco S, Orloff LE, Theodore PR (2006) Oklahoma prosthesis: resection of tumor of clavicle and chest wall reconstructed with a custom composite graft. *Ann Thorac Surg* 82:332–334. <https://doi.org/10.1016/j.athoracsur.2005.09.029>
- Wang L, Cao T, Li X, Huang L (2016) Three-dimensional printing titanium ribs for complex reconstruction after extensive posterolateral chest wall resection in lung cancer. *J Thorac Cardiovasc Surg* 152:e5–7. <https://doi.org/10.1016/j.jtcvs.2016.02.064>
- Wang L, Kang J, Sun C, Li D, Cao Y, Jin Z (2017) Mapping porous microstructures to yield desired mechanical properties for application in 3D printed bone scaffolds and orthopaedic implants. *Mater Des* 133:62–68. <https://doi.org/10.1016/j.matdes.2017.07.021>
- Weyant MJ et al (2006) Results of chest wall resection and reconstruction with and without rigid prosthesis. *Ann Thorac Surg* 81:279–285. <https://doi.org/10.1016/j.athoracsur.2005.07.001>

Wu YM, Zhang GF, Zhu ZY, Chai Y (2016) Chest wall reconstruction after resection using hernia repair piece. *J Thorac Dis* 8:1353–1355. <https://doi.org/10.21037/jtd.2016.04.25>

Yang CC, Tian XY, Li DC, Cao Y, Zhao F, Shi CQ (2017) Influence of thermal processing conditions in 3D printing on the crystallinity and mechanical properties of PEEK material. *J Mater Process Tech* 248:1–7. <https://doi.org/10.1016/j.jmatprotec.2017.04.027>

Publisher's Note Springer Nature remains neutral with regard to jurisdictional claims in published maps and institutional affiliations.